Effect of NOx and Water Variations on Iodine Loading of AgZ

Nuclear Technology Research and Development

Prepared for
U.S. Department of Energy
Material Recovery and Waste Form Development Campaign

A.T. Greaney, S.H. Bruffey, and R. T. Jubin

Oak Ridge National Laboratory
30 June 2020

SUMMARY

Reprocessing of used nuclear fuel will result in the release of several volatile radionuclides that need to be removed from facility off-gas streams before their release to the environment. Iodine, one of these radionuclides, is expected to be primarily released in the dissolver off-gas stream as iodine (I_2) or methyl iodide (CH_3I). Sorbents that target I_2 and CH_3I removal from the DOG stream will need to adsorb iodine under elevated temperatures and in the presence of water vapor and nitrogen oxides (NO_x). Previous studies examining the adsorption of CH_3I and I_2 in the presence of NO_x gases by silver-exchanged mordenite (AgZ), a zeolite mineral considered for use in this application, have resulted in slightly inconsistent conclusions.

This study characterizes the effects of water vapor, nitric oxide (NO), nitrogen dioxide (NO_2), and operating temperature on the adsorption of both I_2 and CH_3I by AgZ. These effects were determined through the performance of designed factorial experiments allowing the resolution of each variable's effect on iodine loading capacity. These factorial experiments also provide an assessment of whether the variables of interest may have interactions with each other that affect iodine capture by AgZ. The experiments were performed by exposing thin sorbent beds of AgZ to iodine-bearing feed streams. In total, 16 tests were completed.

Of the four variables examined, NO_2 was found to have the most detrimental effect on I_2 and CH_3I adsorption to AgZ: tests including NO_2 in the gas stream resulted in up to a 62% reduction in sorbent capacity. Additionally, because the sorbent capacity was reduced, the sorbent lifetime was also greatly reduced. Tests including NO_2 in the gas stream resulted in up to a 90% reduction in the time-to-sorbent-saturation. Increasing the operating temperature had a slightly detrimental effect on I_2 and CH_3I adsorption by AgZ. The presence of NO or water in the gas stream did not significantly affect adsorption to AgZ.

These results indicate that AgZ used under DOG conditions that include NO_2 will experience significant capacity loss and a shortened sorbent lifetime relative to conditions that do not include NO_2. The information obtained on sorbent saturation capacities and saturation times will be important in assessing the design of potential AgZ-based iodine abatement systems. The chemical reactions underpinning the adsorption of inorganic and organic iodine species by AgZ merit further study, as does the potential for mitigating effects of NO on NO_2 oxidation of Ag^0. The potential for NO_2 transformation or abatement prior to iodine adsorption from the DOG should be considered as a way to improve the lifetime of silver-based sorbents such as AgZ.

This page is intentionally left blank.

CONTENTS

This page is intentionally left blank.

FIGURES

TABLES

This page is intentionally left blank.

ACRONYMS

AgZ   Silver exchanged mordenite

DOG   Dissolver off-gas

NAA   Neutron Activation Analysis

ORNL   Oak Ridge National Laboratory

VOG   Vessel off-gas

This page is intentionally left blank.

EFFECT OF NOx AND WATER VARIATIONS ON IODINE LOADING OF AgZ

1.   INTRODUCTION

1.1   Purpose

The aqueous reprocessing of used nuclear fuel releases four key volatile radionuclides (^{3}H, ^{14}C, ^{85}Kr, and ^{129}I) and some semi-volatile radionuclides such as ^{106}Ru from the used fuel into the off-gas streams of the reprocessing facility. Compliance with US regulations may require that these radionuclides be removed from the off-gas streams before their discharge to the environment (Jubin et al. 2013). These regulations are especially stringent regarding the release of ^{129}I, which has the longest half-life of the radionuclides listed here and can have a significant biological impact. Efficient removal of iodine from facility off-gas streams will be necessary to achieve the required mitigation levels.

Iodine is released during multiple unit operations within the plant and can be found in the shear off-gas, dissolver off-gas (DOG), vessel off-gas (VOG), and waste solidification off-gas streams. An analysis of the distribution of iodine between aqueous separations unit operations found that 95%–99% of total iodine release to the off-gas occurs during dissolution (releasing the iodine into the DOG) and that much of the balance of the iodine is released during solvent extraction (releasing the iodine into the VOG) (Jubin et al. 2013). Iodine is primarily present in the DOG as elemental iodine (I_2), but may also be present as methyl iodide (CH_3I) due to the presence of organics in the recycled nitric acid from the dissolver.

Silver-based minerals, including reduced silver exchanged mordenite (Ag^0Z or AgZ) have been studied as potential iodine sorbents for use in removing iodine from off-gas streams, including the DOG, to meet target decontamination factors. Iodine is suggested to chemically react with the silver to form silver iodide or silver iodate. Some physiosorption is possible as well because of the sizes of the channels in the zeolite crystal structure (Scheele 1983). The DOG is expected to contain iodine at parts-per-million concentration levels, although the concentration may fluctuate significantly during the course of dissolution. As the DOG is associated with a heated nitric acid solution, it will contain water vapor, nitric oxide (NO), and nitrogen dioxide (NO_2) gases. Water vapor will be present at a level dictated by upstream condensers (likely 30°C dew point), and NO_x is likely to be present in the stream at 1%–5% by volume.

This study characterizes the effects of water vapor, NO, NO_2, and operating temperature on the adsorption of both I_2 and CH_3I by AgZ. These effects were determined through the performance of designed factorial experiments allowing the resolution of each variable's effect on iodine loading capacity. These factorial experiments also provide an assessment of whether the variables of interest may have interactions with each other to affect iodine capture by AgZ. The experiments were performed by exposing thin sorbent beds of AgZ to iodine-bearing feed streams.

1.2   Background

Previous studies examining the adsorption of CH_3I and I_2 by AgZ in the presence of NO_x gases have resulted in slightly inconsistent conclusions. Thomas et al. (1977) studied the effects of water vapor, NO, and NO_2 on I_2 loading on AgZ buy running air streams at 15 m/min through a 15 cm deep sorbent bed at 150°C with 1.5 ppm I_2. Humidity tests were completed with 6% water, and NO_x tests were completed with 2% NO_x. They concluded that the presence of NO increases I_2 loading, the presence of NO_2 decreases I_2 loading, and the presence of water has no significant impact. They suggested that NO_2 may partially oxidize the silver to reduce the effectiveness of the sorbent.

Jubin (1980, 1982) performed a series of tests to study the effects of temperature, water vapor, NO, and NO_2 on the loading of CH_3I on AgZ. In these tests, between 0.5 and 1 ppm CH_3I was flowed over a series of six 2.54 cm thick beds. The air stream was held at either −54°C or 34°C dew point, NO concentration

was either 0% or 3%, and NO_2 concentration was either 0% or 1.4%. The bed temperature was varied between 100°C and 225°C. Iodine loading was measured as ^{131}I using a NaI detector. From these tests, higher operating temperatures (200°C) and added moisture improved CH_3I loadings, although the presence of NO and NO_2 did not have a significant effect.

Scheele et al. (1983) performed deep bed studies of CH_3I and I_2 loading on AgZ at 110°C, 150°C, and 225°C with water, NO, NO_2, or a combination thereof present. Iodine loading was measured using X-ray fluorescence. They found that with NO or NO_2 present, CH_3I was converted to I_2. The presence of water improved loadings onto the sorbent, whereas temperature, NO, and NO_2 did not have a discernible effect.

Recently, Bruffey and Jubin (2014) and Bruffey et al. (2019) tested the effects of humid air and NO_x (833 ppm NO + 833 ppm NO_2) on CH_3I loading on a thin bed of AgZ. These studies found that a 43% reduction in iodine capacity occurs when NO_x is present, and a 23% reduction in iodine capacity occurs when NO_x and water are present in the gas stream. Thus, the presence of NO_x impedes CH_3I adsorption by AgZ. The addition of water may reduce the effects of oxidation by interacting with the NO_x.

These previous studies show some conflicting effects of different components on iodine adsorption. This may be a result of different analytical methods for quantifying adsorption. In this study, the effects of temperature (135°C and 165°C), water vapor (−70°C and 0°C dew point), and NO_x gases (0% and 1% NO and NO_2) on I_2 and CH_3I loading on AgZ were examined and iodine loading quantified using neutron activation analysis.

2. MATERIALS AND METHODS

2.1 Thin Bed Test Design

Silver mordenite was obtained from Molecular Products in an engineered pelletized form (Ionex-Type Ag 900 E16). It contains 9.5 wt% silver and has a 0.16 cm pellet diameter. Before use in testing, the sorbent material was reduced by exposure to a 4% H_2 blend in nitrogen at 270°C for 10 days. After reduction, the material was stored under argon to limit oxidation by air. Details of this procedure are provided by Anderson et al. (2012). One batch of AgZ was reduced for the I_2 tests and another batch was reduced for the CH_3I tests, both following the procedure above.

Thin bed testing of CH_3I and iodine adsorption by AgZ was performed using a custom-built thermogravimetric analyzer (TGA) (Figure 1). A thin bed of sorbent material (~2 g total weight) was contained within a temperature-controlled oven. This thermogravimetric analyzer is designed to weigh the sorbent continuously as the sorbent is exposed to a gas stream bearing the components of interest. Humid air, NO, and NO_2 were added to the feed gas. The TGA allows for the iodine loading of the sorbent to be observed in real-time. Once the weight gain was observed to be less than 5 mg/g for a 24 hour period, the sorbent was assumed to be saturated. It was then purged with dry air for 24 hours to remove any physiosorbed iodine.

A 50 ppm CH_3I-bearing feed stream was generated by sparging liquid CH_3I with N_2 at a known flow rate. The CH_3I was contained within a freezer at -33°C to depress the vapor pressure to the levels required for generating low concentration gas streams. A 25 ppm I_2 stream was generated by flowing dry air through a bed of iodine crystals at a known flow rate and temperature. The concentrations were selected to provide equivalent moles of iodine to the sorbent for both sorbates. NO and NO_2 gas were procured commercially. Humid air was generated by sparging liquid water with a dry gas stream at a known flow rate and temperature. The dry gas stream for generating humid air, gaseous I_2, and balancing flow rates was dried to −70°C before contacting the test system.
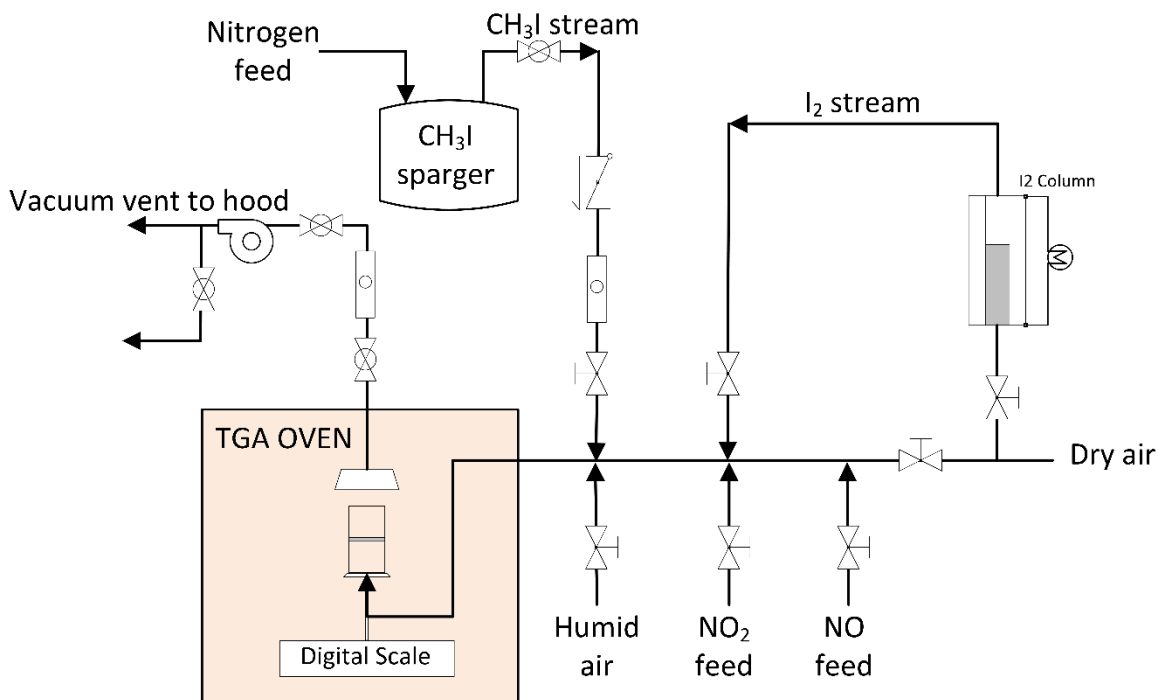
Figure 1: Simplified test system schematic

2.2   Test Matrix

Eight tests were planned using a fractional factorial design to test four factors with two-levels: temperature (135°C or 165°C), NO concentration (0% or 1%), NO_2 concentration (0% or 1%), and the presence of humid air (dew point of -70°C or 0°C) (Table 1). Thus, each level of each variable was tested four times. Each series of eight tests were completed with 50 ppm CH_3I and 25 ppm I_2, for a total of 16 tests. The test design and analysis were informed by Davies, 1967.

Table 1: Designed factorial experiment

Run no.	Temp. (°C)	[NO] (%)	[NO$_2$] (%)	Dew Point (°C)
1	135	0	0	-70
2	165	0	0	0
3	135	1	0	0
4	165	1	0	-70
5	135	0	1	0
6	165	0	1	-70
7	135	1	1	-70
8	165	1	1	0

2.3   Iodine Concentration Analysis

After test completion, the final loading weight was recorded and samples were removed from the TGA system by vacuum and sent to ORNL's High Flux Isotope Reactor for neutron activation analysis (NAA) for adsorbed iodine. Each sample was irradiated for ~10 seconds.

3. RESULTS

The CH₃I and iodine test results are presented in Tables 2 and 3, respectively. The total loading is listed in the mg I/g (milligrams of iodine per gram) sorbent columns as estimated by the TGA and confirmed by NAA. The TGA data are primarily used to indicate the end of loading and may reflect the adsorption of non-iodine species, while the NAA data are a more accurate representation of total iodine adsorption. The "time to saturation" column lists the approximate time to loading curve plateaus, rounded to the nearest hour. The "loading rate" column lists the average rate of sorbent mass gain to the time of saturation, estimated using the TGA data.

Table 2: Methyl iodide results estimated gravimetrically by the TGA and measured using NAA.

Run #	Test ID	Temp. (°C)	[NO] (%)	[NO₂] (%)	Dew Point (°C)	TGA	NAA	Time to Saturation (hr)	Loading Rate (mg/g/hr)
						(mg I / g sorbent)			
1	FY19-001	135	0	0	-70	85.6	**90.3 ± 2.5**	255	0.33
2	FY20-017	165	0	0	0	105	**101.4 ± 2.2**	138	0.87
3	FY20-020	135	1	0	0	89	**83.8 ± 2.4**	166	0.61
4	FY20-021	165	1	0	-70	44	**52.6 ± 2.0**	57	0.85
5	FY20-018	135	0	1	0	46	**33.2 ± 4.4**	30	2.28
6	FY19-009	165	0	1	-70	35	**37.3 ± 2.1**	72	0.57
7	FY19-011	135	1	1	-70	74	**75.2 ± 2.1**	219	0.34
8	FY20-022	165	1	1	0	45	**55.9 ± 2.0**	85	0.730

Table 3: Iodine results estimated gravimetrically by the TGA and measured using NAA.

Run #	Test ID	Temp. (°C)	[NO]	[NO₂]	Dew Point (°C)	TGA	NAA	Time to Saturation (hr)	Loading Rate (mg/g/hr)
						(mg I / g sorbent)			
1	FY17-034	135	0%	0%	-70	67	**68.7 ± 0.0***	83	0.84
2	FY17-028	165	0%	0%	0	60	**64.8 ± 1.0**	57	1.11
3	FY17-031	135	1%	0%	0	87	**88.5 ± 0.0***	88	1.09
4	FY17-032	165	1%	0%	-70	60	**58.5 ± 0.0***	76	0.76
5	FY20-014	135	0%	1%	0	57	**38.0 ± 4.3**	60	1.14
6	FY20-010	165	0%	1%	-70	50	**18.5 ± 0.4**	119	0.46
7	FY20-009	135	1%	1%	-70	48	**36.8 ± 1.6**	78	0.93
8	FY20-013	165	1%	1%	0	48	**46.4 ± 5.3**	107	0.55

*Error was <0.1%.

3.1 Loading Rates

Including a purge period at the end of the run, tests took between 80 and 300 hours to complete (Figures 2 and 3; Appendix A). The time to sorbent saturation during CH₃I loading ranges from 30 to 255 hours and the time to sorbent saturation during I₂ loading ranges from 57 hours to 199 hours. Generally, CH₃I absorbs more slowly than I₂ (Figure 4; Appendix A). Additionally, CH₃I loading rates vary more with changing test conditions; I₂ loading rates are more constant.

3.1.1   CH₃I Loading Rates

Methyl Iodide test #1 follows a linear loading curve and is the only CH_3I test condition that does not include humid air or NO_x gas in the feed stream (Figure 2). The remaining seven tests generally follow exponential curves on a multiday timescale. Additionally, CH_3I Test #1 resulted in the longest time to sorbent saturation (Table 2, Figure 4), so the presence of humid air and NO_x changes the shape of the loading curve and decreases the time to sorbent saturation. When the first few hours of loading are considered (lower panel, Figure 2), three tests (#3, #5, and #8) quickly gain > 30 mg/g sorbent within the first hour of loading before the loading rate slows; these three tests had a humid air stream and either one or both NO_x species were present. CH_3I Test #2, including humid air but no NO_x, only gained ~12 mg/g sorbent within the first hour of loading.

3.1.2   I₂ Loading Rates

Loading rates were estimated with the TGA, therefore the data should be interpreted as such (e.g. the coadsorption of water or NO_x species is also recorded). All I_2 tests follow a generally exponential loading curve on a multiday timescale (upper panel, Figure 3). There is generally less variability between the time to sorbent saturation for each test as compared to testing performed with CH_3I, with six of the eight tests reaching saturation within 31 hours of each other (between 57 and 88 hours). Only Tests #6 and #8 fall outside of this window, taking more than 100 hours to reach saturation (Table 2, Figure 4). When the first few hours of loading are considered (lower panel, Figure 3), five tests (#3, #5, #6, #7, #8) quickly gain > 23 mg/g sorbent in the first hour of loading before the loading rate slows; these include the four tests with NO_2 present and the test with a combination of humid air and NO present. This may reflect the uptake of water or formation of oxidized Ag compounds on the mordenite instead of iodine uptake, but further studies are needed to confirm this. The other three tests (#1, #2, #4) show an initially slower loading rate and either have no NO_x present or have only NO present in a dry air stream. These three tests with no NO_x or only NO in a dry air stream show a very constant loading rate for the first 48 hours (Figure 3), and result in similar final concentrations of absorbed iodine.

For both CH_3I and I_2 species, Test #1 (no humidity or NO_x) has the slowest initial loading rate during the first few hours, which would be expected because the water saturation capacity for AgZ is reached within hours when humidity is present in the feed stream. Additionally, the loading rate of Test #5 (135°C, 1% NO_2, humid air stream) shows similar patterns for both I_2 and CH_3I: loading stalls within the first 10 min, quickly gains the most mass of any test within the first few hours, and ultimately saturates the quickest with the lowest final concentration of absorbed iodine (dark green curve on Figures 2 and 3).
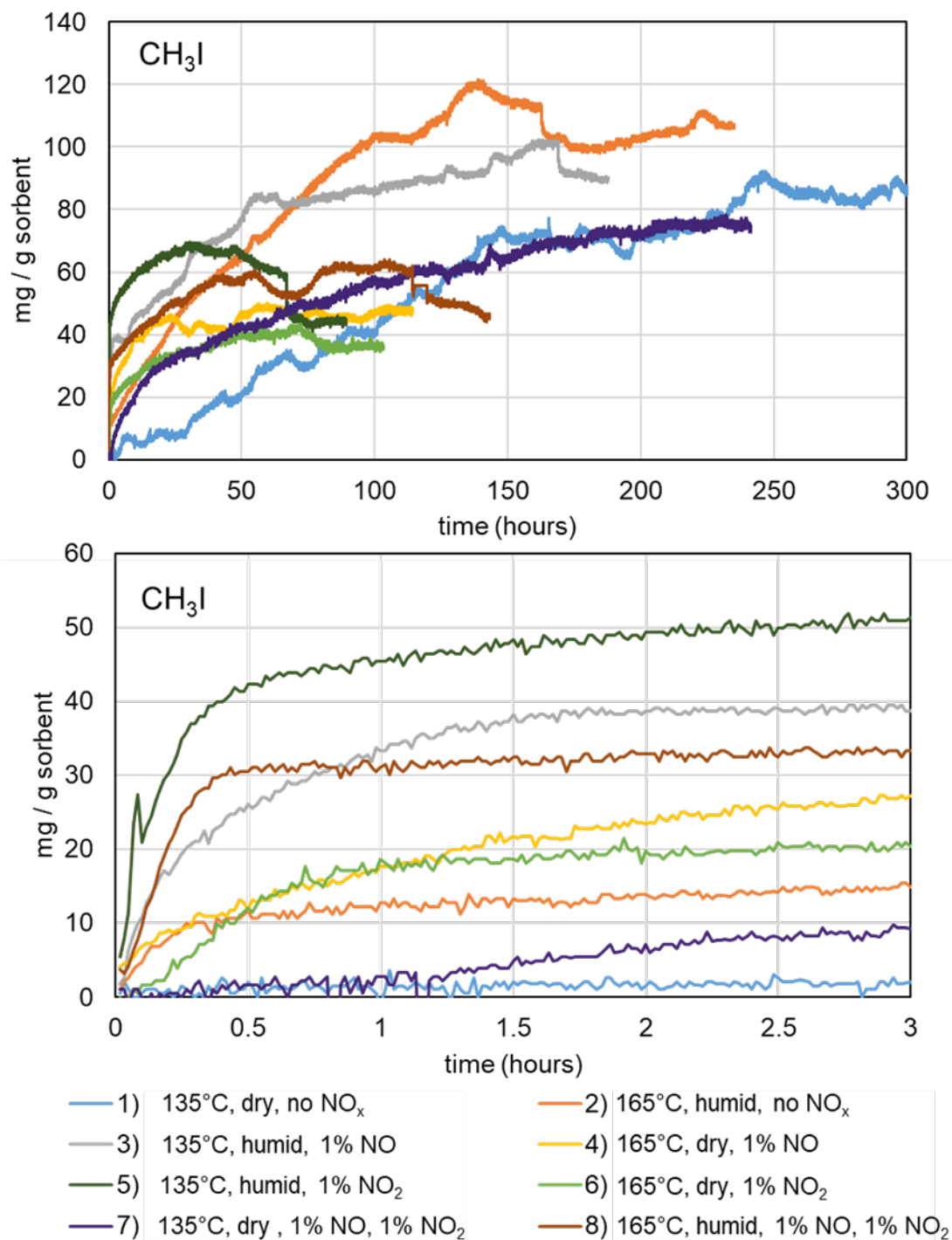
Figure 2: CH$_3$I loading curves from eight tests. *Above*, entire run; *below*, first three hours of loading.
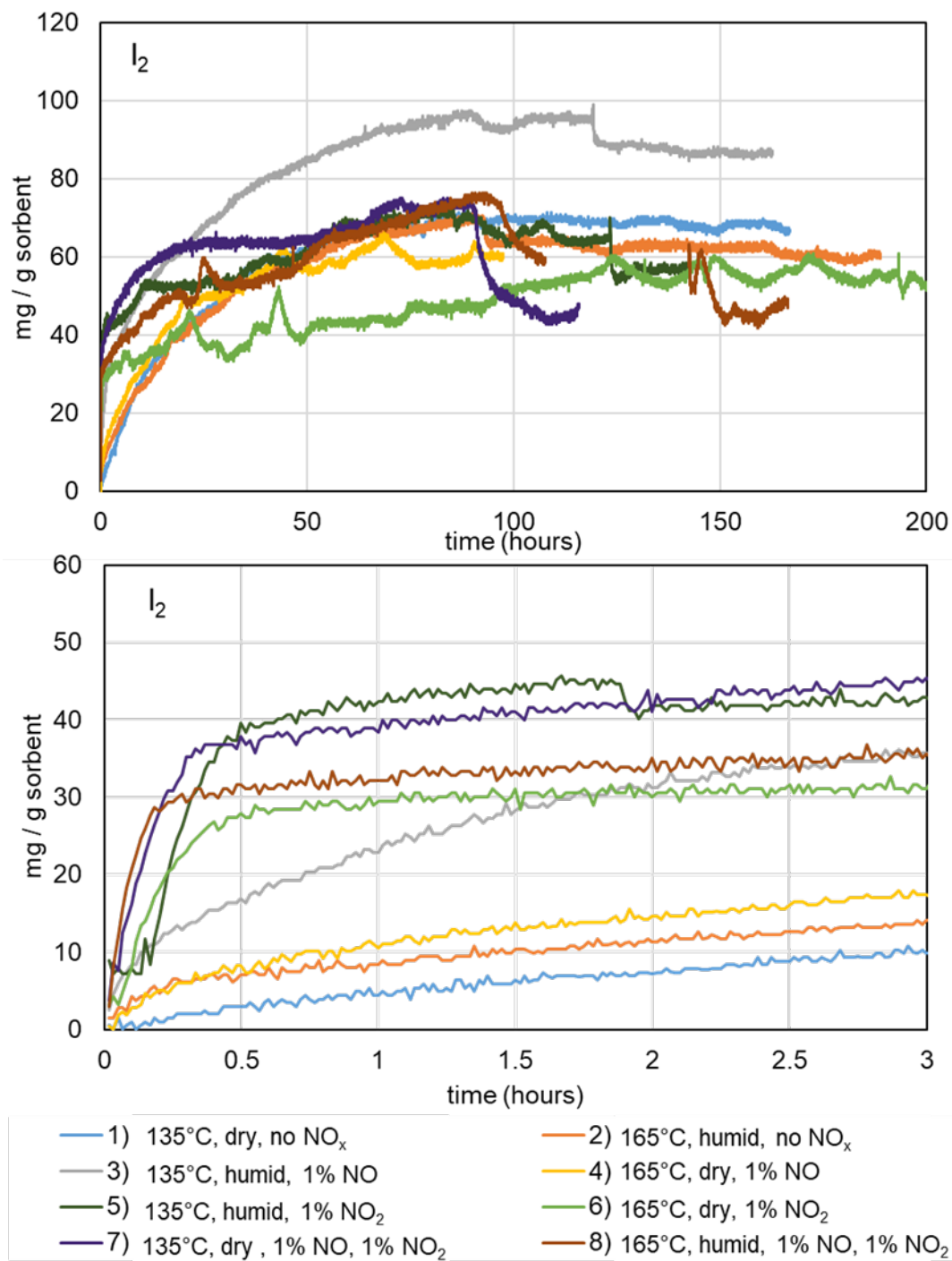
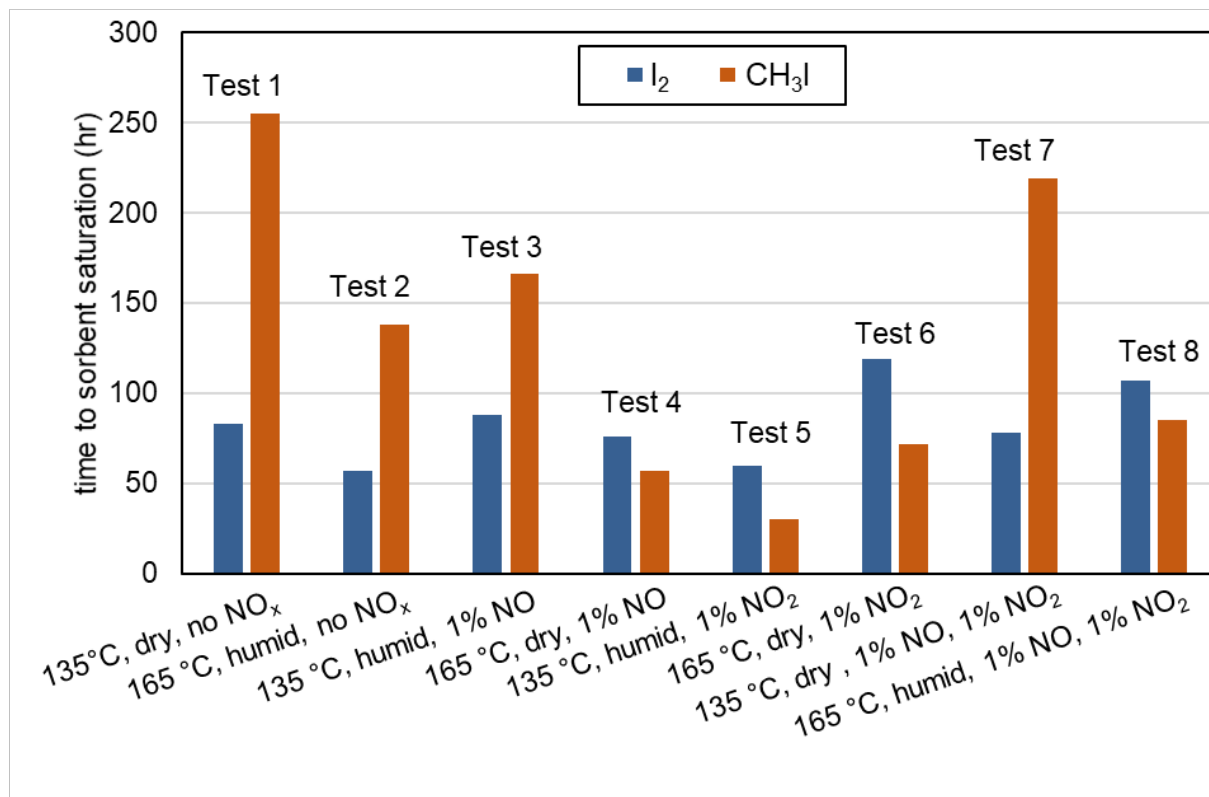Figure 3: I$_2$ loading curves from eight tests. *Above*, entire run; *below*, first three hours of loading.

Figure 4: Approximate time to sorbent saturation in hours, determined by the time at which the loading curve plateaus. CH$_3$I results are in orange, I$_2$ results are in blue.

3.2   Sorbent capacity

3.2.1   CH$_3$I retention

Methyl iodide test #1 established a baseline sorbent capacity of 90 mg I / g sorbent (dashed orange line, Figure 5). Test #2 (165°C, humid air stream) resulted in higher iodine retention of 101 mg I/ g sorbent. Test #3 (135°C, 1% NO, humid air stream) resulted in 84 mg I / g sorbent which is 92% of the capacity of Test #1. Test #7 (135°C, 1% NO, 1% NO$_2$) resulted in 75 mg I/g sorbent which is 83% of the capacity of Test #1. Tests #4 (165°C, 1% NO) and #8 (165°C, 1% NO, 1% NO$_2$, humid air) resulted in approximately 60% of the capacity of Test #1. Tests #5 (135°C, 1% NO$_2$, humid air) and #6 (165, 1% NO$_2$) resulted in ≤40% of the capacity of Test #1. Thus, the tests that include solely NO$_2$ resulted in the most reduced sorbent capacity.

3.2.2   I$_2$ retention

Iodine test #1 established the baseline sorbent capacity 69 mg I / g sorbent (dashed blue line, Figure 6). Test #2 (165°C, humid air stream) resulted in 65 mg I/ g sorbent, which is almost 100% of the capacity of Test #1. Test #3 (135°C, 1% NO, humid air stream) resulted in an increased sorbent capacity compared to Test #1 of 88 mg I / g sorbent. Test #4 (165°C, 1% NO) resulted in 85% of the capacity of Test #1. Test #8 (165°C, 1% NO, 1% NO$_2$, humid air) resulted in approximately 68% of the capacity of Test #1. Tests #5 (135°C, 1% NO$_2$, humid air) and #7 (135°C, 1% NO, 1% NO$_2$) resulted in approximately 55% of the capacity of Test #1. Test #6 (165, 1% NO$_2$) resulted in 27% of the capacity of Test #1.
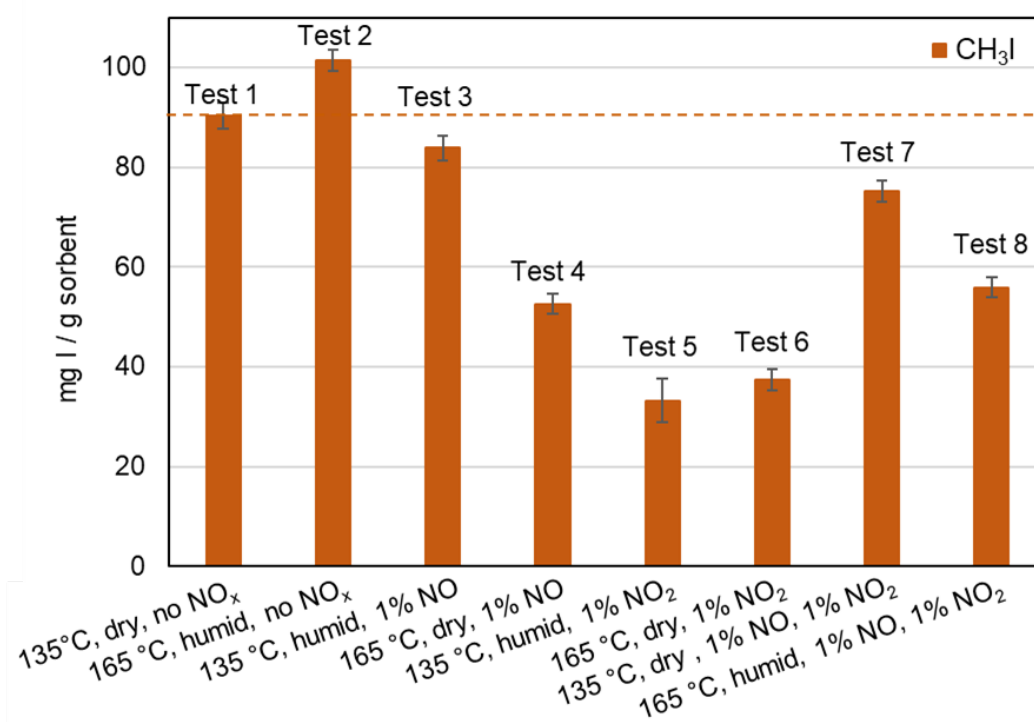
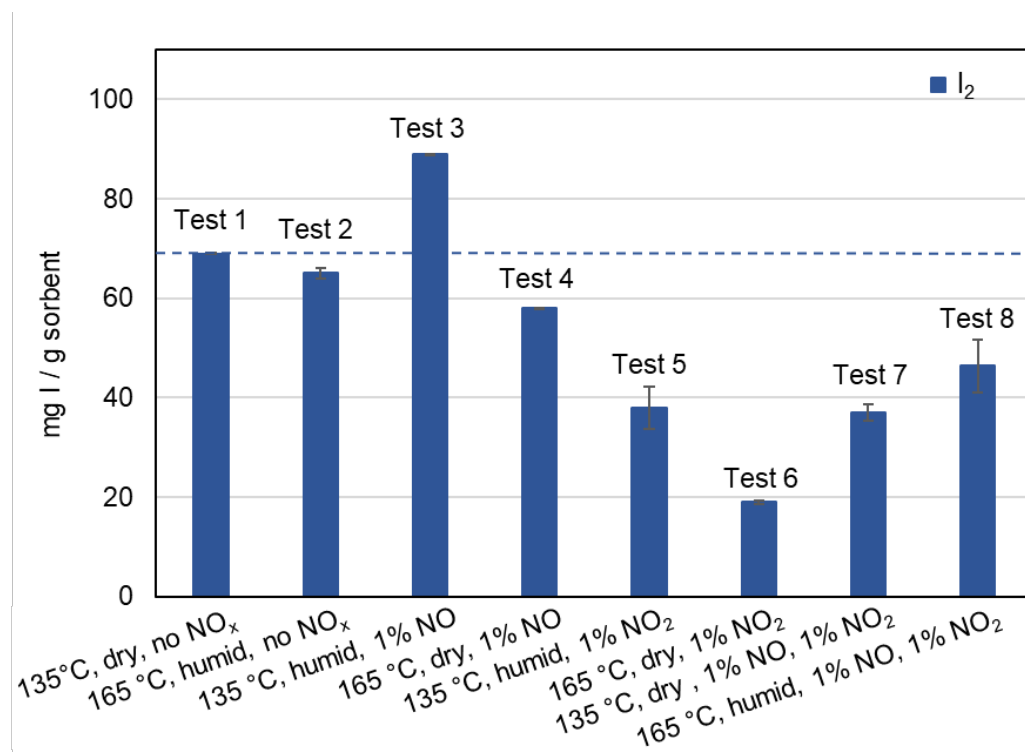Figure 5: Total retained iodine in milligrams of iodine per gram (mg I/g sorbent) for CH$_3$I loading.

Figure 6: Total retained in milligrams of iodine per gram (mg I/g sorbent) for I$_2$ loading.

3.3 Results of Designed Factorial Experiment

Analysis of the observed iodine loadings was performed as described in Davies, 1967 and the results are shown in Table 4. In short, for each variable, the summed loadings of the four tests that did not include that variable were subtracted from the summed loadings of the four tests that did include the variable. This difference was divided by the number of variables tested and resulted in the calculated "effect" for each individual variable, which is a unitless parameter. The final iodine loading (or maximum iodine capacity under the selected conditions) as measured by NAA was used to calculate the magnitude of any effects. In this fractional factorial design, the effects of four variables and three two-factor interactions can be determined. In Table 4, the second-order effects of interactions between two variables can be calculated on either the first set of listed variables or the second set (e.g. interactions between temperature and NO *or* interactions between NO_2 and water). The results must be considered in context of the individual variable effects and are interpreted in the text. The expected variance for replicate TGA tests is ±7 mg I/g AgZ in measured capacity, as estimated using the data here and from replicate tests performed in Bruffey and Jubin (2015). Thus, effects of greater magnitude than ±7 are expected to be statistically significant (Table 4).

For both CH_3I and I_2 adsorption by AgZ, it was observed that of the four variables studied, the presence of NO_2 in the gas stream had the largest effect, depressing iodine loading significantly (Figure 7). Increased temperature was observed to result in a slightly depressed loading for both species.

The presence of NO and water in the gas stream had negligible effects independently for CH_3I adsorption by AgZ. Synergistic interactions between variables were analyzed and interpreted in the context of the individual variable effects. It was found that CH_3I adsorption by AgZ was negatively affected when both water and NO_2 were present and positively influenced when water was present at a loading temperature of 165°C. No interactions between NO and water or temperature and NO_2 were observed for CH_3I adsorption by AgZ (Table 4).

In the case of I_2 adsorption by AgZ, the presence of NO and water in the gas stream was observed to independently result in slightly increased loading. Synergistic interactions between variables were analyzed, but no second order effects were found to be statistically significant (Table 4).

Table 4: Results of factorial experimental analysis. Effects greater than ±7 are considered significant.

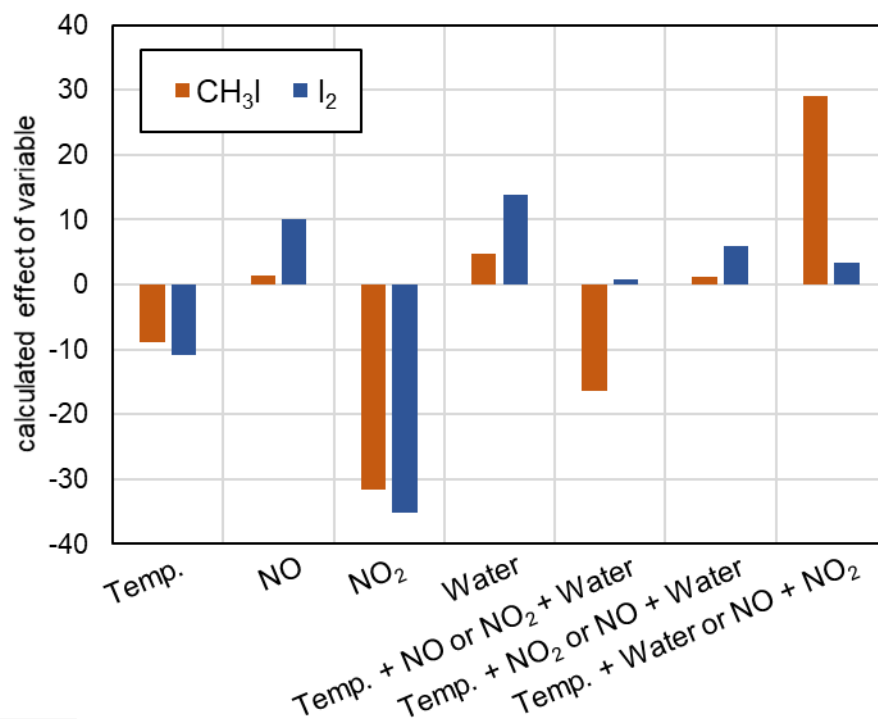| Variable	CH$_3$I		I$_2$	
	Effect	**Significance**	**Effect**	**Significance**
Temperature	−9	Decreases loading	−11	Decreases loading
NO	1	No effect	10	Increases loading
NO$_2$	−32	Decreases loading	−35	Decreases loading
Water	5	No effect	14	Increases loading
(Temp., NO) *or* (NO$_2$, Water)	−16	Decreases loading	1	No interaction
(Temp., NO$_2$) *or* (NO, Water)	1	No interaction	6	No interaction
(Temp., Water) *or* (NO, NO$_2$)	29	Increases loading	3	No interaction

Figure 7: Results of factorial experimental analysis. Statistical significance is ±7 as calculated by replicate experiments.

4.   DISCUSSION

4.1   Effects on sorbent capacity

NO_2 gas has the most significant impact on I_2 and CH_3I adsorption by AgZ (Figure 7). The adsorption of both species was significantly negatively influenced by the presence of 1% NO_2 in the gas stream. Tests that included NO_2 showed up to a 62% reduction in sorbent capacity compared to baseline test conditions (Figures 5 and 6). The NO_2 likely oxidizes Ag^0 to Ag^{1+}, forming Ag_2O and decreasing reactivity with iodine on the zeolite (Scheele et al. 1983). The high interaction effect calculated between NO and NO_2 on CH_3I loading (last line, Table 4) may suggest that the addition of NO in the gas stream with NO_2 mitigates the oxidizing effects of NO_2 on silver, thereby facilitating the formation of AgI and $AgIO_3$ (Table 5). These findings support those of Thomas et al. (1977). Additionally, it appears that interactions between NO_2 and water may also depress CH_3I loading, but further studies are needed to fully assess second and third order interactions between variables.

Increasing the temperature from 135°C to 165°C was also found to slightly negatively affect I_2 and CH_3I adsorption by AgZ, although the magnitude of this effect is less than that of NO_2. These findings contrast with the findings of Jubin (1981, 1983) who found 200°C to be the optimized loading temperature. This discrepancy may be due to the fact that this study removed physiosorbed iodine by purging the system with dry air after the loading curve had plateaued.

The presence of water and NO independently had no significant influence on CH_3I loading, but they did slightly increase I_2 loading. The presence of NO in the air stream may keep silver from being oxidized by NO_2, thereby facilitating the formation of silver iodide and iodate. Thermodynamic calculations show that the presence of NO in the air stream will indeed result in a lower Gibbs free energy of formation of AgI and $AgIO_3$ relative to reactions involving NO_2 (Table 5). This result is in accordance with Thomas et al (1977) who found that NO improved loading of I_2. Similarly, the presence of water in the gas stream may

work to mitigate the effects of Ag oxidation by NO_2. These results are in accordance with data presented in Bruffey et al. (2019) who found that NO_x alone decreases loading by 43%, relative to baseline measurements. However, when humid air was added to the NO_x stream, loading only decreased by 23%, relative to baseline measurements, suggesting humid air may improve iodine loading onto AgZ.

Table 5: Gibbs free energies of relevant reactions involving NO and NO_2, from Scheele et al. (1983).

Reaction	ΔG (kJ/mol Ag)
$2 Ag + I_2 + 3 NO \leftrightarrow AgI + AgIO_3 + 3/2 N_2$	-223.3
$2 Ag + I_2 + 3/2 NO_2 \leftrightarrow AgI + AgIO_3 + 3/4 N_2$	-132.1

4.2   Effects on loading rate

The baseline conditions of Test #1 established that CH_3I adsorbs to AgZ approximately three times more slowly than I_2 (Figure 4). However, once additional components were introduced into the gas stream, the time to sorbent saturation became similar for the two iodine species. This may be because the presence of NO and water together appears to increase the iodine capacity on the AgZ. Additionally, the presence of NO_2 in the gas stream resulted in a diminished time-to-sorbent-saturation for CH_3I loading in all tests involving NO_2 except for Test #7 where NO was also present in the gas stream. Thus, NO_2 effectively decreases sorbent capacity and reduces the lifetime of the sorbent by up to 90% (e.g., CH_3I Test# 5: 30 hours to sorbent saturation vs. 255 hours for the baseline Test #1, Figure 4).

5.   CONCLUSIONS

A fractional factorial experiment examining the effects of NO_2, NO, water, and operating temperature on the adsorption of CH_3I and I_2 by AgZ was conducted. Given the comparison between the data presented in this study and that from the literature, it is clear that the presence of NO_2 in the gas stream is the most significant factor in reducing the total capacity and lifetime of AgZ as an iodine sorbent. For streams high in NO_2 concentration, such as the DOG, AgZ will function less efficiently than when deployed for streams low in NO_2, such as the VOG. Slightly negative impacts of higher operating temperature on sorbent capacity were observed, so it is recommended that sorbent beds be kept below 165°C. At the timescales studied here (<300 hours), NO and water alone have a negligible effect on sorbent capacity and loading rate, but may work to mitigate the negative effects of NO_2.

The chemical reactions underpinning the adsorption of inorganic and organic iodine species by AgZ merit further study, as does the potential for mitigating effects of NO on NO_2 oxidation of Ag^0. The potential for NO_2 transformation or abatement before iodine adsorption from the DOG should be considered as a way to improve the lifetime of silver-based sorbents such as AgZ.

6.   REFERENCES

Anderson, K. K., S. H. Bruffey, D. L. Lee, R. T. Jubin, and J. F. Walker. 2012. Iodine Loading of Partially Reduced Silver Mordenite. Report no. FCRD-SWF-2013-000079, US Department of Energy Separations and Waste Forms Campaign, December 28.

Bruffey, S. H. and R. T. Jubin. 2014. *Complete Phase 1 tests as described in the multi-lab test plan for the evaluation of CH$_3$I adsorption on AgZ.* Report No. FCR&D-SWF-2014-000280, US Department of Energy Separations and Waste Forms Campaign, September.

Bruffey, S. H. and R. T. Jubin. 2015. Initial Evaluation of Effects of NO$_x$ on Iodine and Methyl Iodide Loading of AgZ and Aerogels, Report no. FCRD-SWF-2015-0000426, US Department of Energy, March 31.

Bruffey, S. H., A. T. Greaney, R. T., Jubin, N. R. Soelberg, and A. Welty. 2019. Iodine Retention of Longchain Organic Iodides on Silver-based Sorbents under DOG and VOG Conditions, Oak Ridge National Laboratory, Oak Ridge, TN.

Davies, O. L. (Editor). 1967. *Design and Analysis of Industrial Experiments*, 2nd ed. Hafner Publishing Company, New York.

Jubin, R. T. 1981. "Organic Iodine Removal from Simulated Dissolver Off-Gas Streams Using Silver-Exchanged Mordenite," 16th DOE Nuclear Air Cleaning Conference

Jubin, R. T. 1983. "Organic Iodine Removal from Simulated Dissolver Off-Gas Streams Using Partially Exchanged Silver Mordenite," 17th DOE Nuclear Air Cleaning Conference

Jubin, R. T., D. M. Strachan, and N. R. Soelberg. 2013. Iodine Pathways and Off-Gas Stream Characteristics for Aqueous Reprocessing Plants—A Literature Survey and Assessment, Report nos. FCRD-SWF-2013-000308, ORNL/LTR-2013/383, INL/EXT-13-30119, September 15.

Scheele R. D., L. L. Burger, C. L. Matsukazi. 1983. Methyl Iodide Sorption by Reduced Silver Mordenite, PNL-4489, US Department of Energy.

Thomas T. R., B. A. Staples, and L. P. Murphy. 1977. "The Development of AgZ for Bulk ^{129}I removal from Nuclear Fuel Reprocessing Plants and Pb$_X$ for ^{129}I Storage," 15th DOE Nuclear Air Cleaning Conference

This page is intentionally left blank.

Appendix A
Loading Curves For Tests #1–8

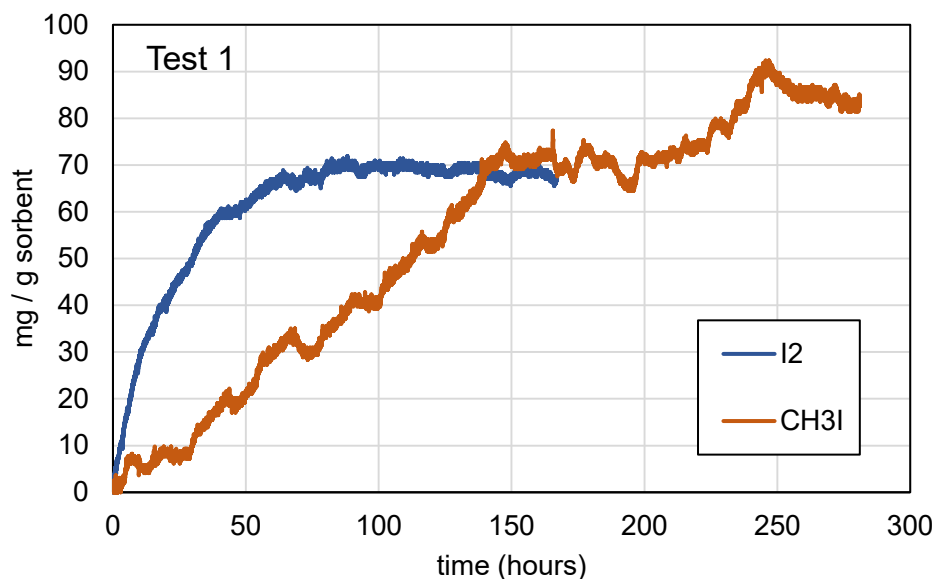Loading curves of CH_3I and I_2 are presented for each individual test.

Figure A1. Loading curve for Test 1: 135°C, dew point -70°C, 0% NO, 0% NO$_2$.
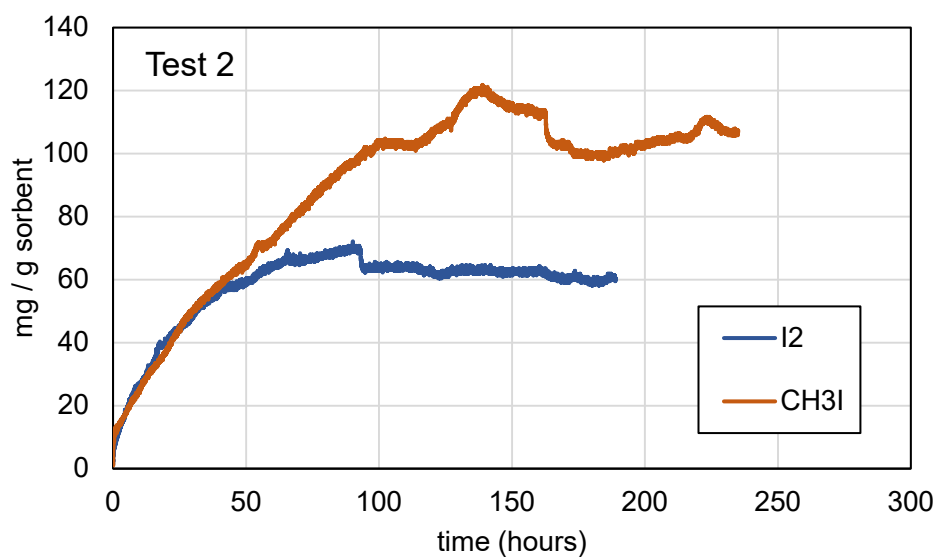

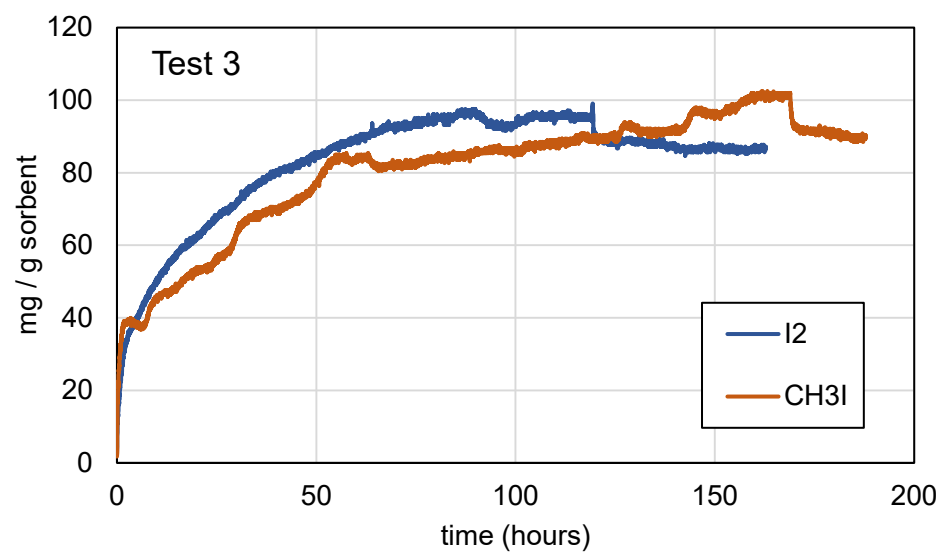**Figure A2.** Loading curve for Test 2: 165°C, dew point 0°C, 0% NO, 0% NO$_2$.

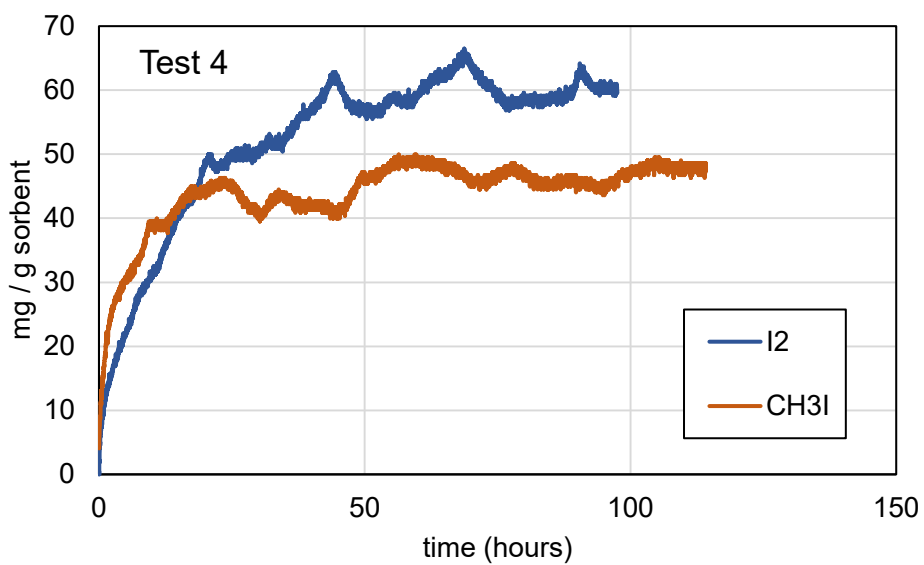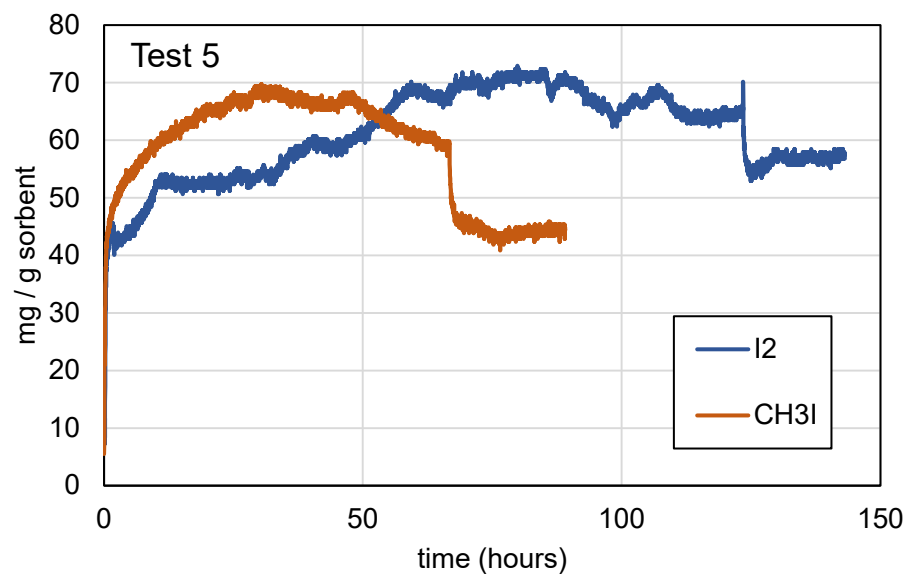**Figure A3.** Loading curve for Test 3: 135°C, dew point 0°C, 1% NO, 0% NO$_2$.

Figure A4. Loading curve for Test 4: 165°C, dew point -70°C, 1% NO, 0% NO$_2$.

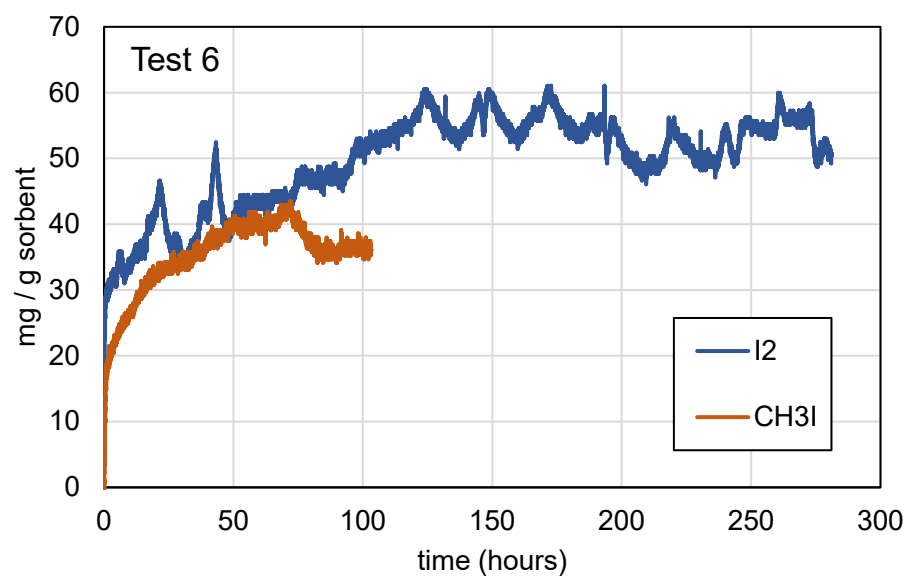**Figure A5.** Loading curve for Test 5: 135°C, dew point 0°C, 0% NO, 1% NO$_2$.

Figure A6. Loading curve for Test 6: 165°C, dew point -70°C, 0% NO, 1% NO$_2$.

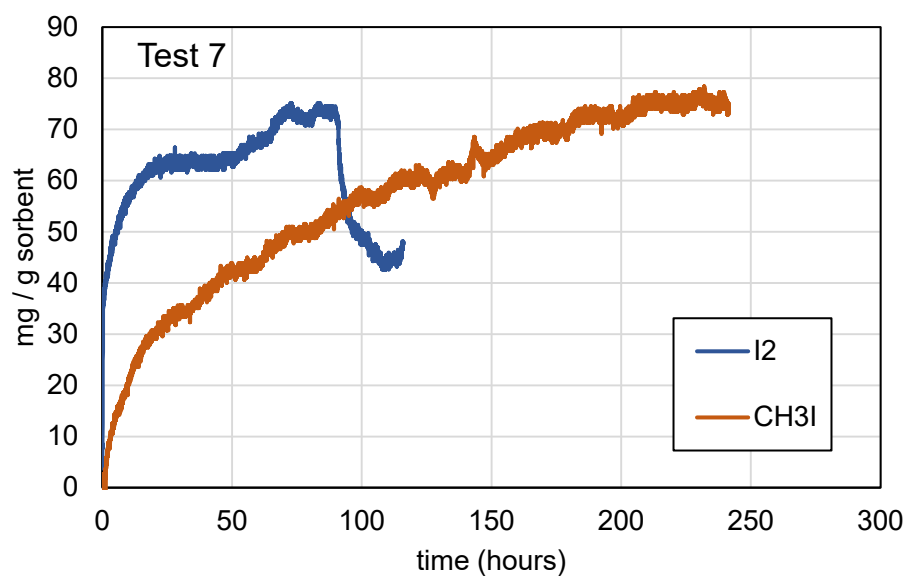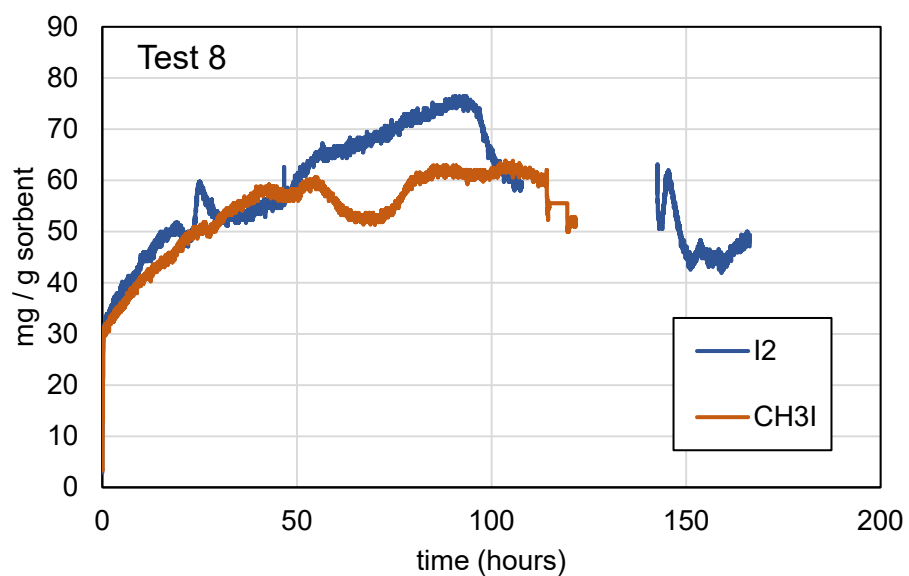**Figure A7.** Loading curve for Test 7: 135°C, dew point -70°C, 1% NO, 1% NO$_2$.

Figure A8. Loading curve for Test 8: 165°C, dew point 0°C, 1% NO, 1% NO$_2$.